

Sustainable Transparency in Recommender Systems: Bayesian Ranking of Images for Explainability

JORGE PAZ-RUZA, AMPARO ALONSO-BETANZOS, BERTA GUIJARRO-BERDIÑAS, BRAIS CANCELA, and CARLOS EIRAS-FRANCO, Universidade da Coruña, CITIC, Spain

Recommender Systems have become crucial in the modern world, commonly guiding users towards relevant content or products, and having a large influence over the decisions of users and citizens. However, ensuring transparency and user trust in these systems remains a challenge; personalized explanations have emerged as a solution, offering justifications for recommendations. Among the existing approaches for generating personalized explanations, using visual content created by the users is one particularly promising option, showing a potential to maximize transparency and user trust. Existing models for explaining recommendations in this context face limitations: sustainability has been a critical concern, as they often require substantial computational resources, leading to significant carbon emissions comparable to the Recommender Systems where they would be integrated. Moreover, most models employ surrogate learning goals that do not align with the objective of ranking the most effective personalized explanations for a given recommendation, leading to a suboptimal learning process and larger model sizes. To address these limitations, we present BRIE, a novel model designed to tackle the existing challenges by adopting a more adequate learning goal based on Bayesian Pairwise Ranking, enabling it to achieve consistently superior performance than state-of-the-art models in six real-world datasets, while exhibiting remarkable efficiency, emitting up to 75% less CO₂ during training and inference with a model up to 64 times smaller than previous approaches.

CCS Concepts: • **Information systems** → **Recommender systems**; • **Computing methodologies** → **Learning to rank**; *Transfer learning*; • **Social and professional topics** → **Sustainability**.

Additional Key Words and Phrases: Machine Learning, Explainable Artificial Intelligence, Recommender Systems, Sustainable Machine Learning, Explainable Recommendations, Image-based Explainability

1 INTRODUCTION

In recent years, the field of Artificial Intelligence (AI) has witnessed a significant rise in the development, research, and deployment of complex AI systems that can have a direct impact on users' and citizens' lives. From decision-making processes to personalized recommendations, they have become necessary components of numerous applications and fields, enhancing user experience and improving the communicative capabilities of institutions and companies. However, as these systems grow in complexity and influence on society, there is a pressing need to ensure their transparency and explainability, particularly in domains where user trust is paramount [7].

The growing importance of explainability in AI systems during the past decade stems from the need to address the “black box” nature of many complex models [18], as users often find it challenging to comprehend why an AI system produces a specific output, such as an item or product recommendation provided by a Recommender System. This lack of transparency has proved to lead to a diminished user experience, reduced trust from society in AI systems, and, in the worst case, potentially harmful outcomes [9]. This has popularly led to regulatory efforts to ensure transparency and accountability in AI systems. For instance, the European Union's General Data Protection Regulation (GDPR) mandates the right to explanation in data-treating systems, granting users insight into any automated decisions made by them [22]. Ethical-oriented guidelines, such as those published by the EU's High-Level Expert Group on Artificial Intelligence, emphasize

transparency and accountability in AI [14]. Additionally, the U.S. Federal Trade Commission (FTC) emphasized the need for explainable AI to prevent deceptive practices in a recent report [5].

With respect to recommendations, the increasing reliance of businesses and users on AI-based Recommender Systems (RS) means that understanding and interpreting the recommendations provided to users has become crucial. Users expect personalized recommendations that align with their preferences, but they also desire explanations for why certain recommendations are made, e.g. due to a lack of quality of the recommendation or mistrust in the system; as such, explaining the outputs of RS not only enhances user trust, but also further enables users to make informed decisions, promoting a more interactive and engaging user experience [24].

In the quest for explainability, one promising avenue is leveraging the visual content associated with AI inputs and outputs. Visual information, such as images, plays a vital role in human perception and decision-making processes, having been explored before as a tool for explainability in other tasks [23]. In the context of user-to-item recommendations, among other examples, Netflix uses a small selection of movie thumbnails crafted by experts to cater to different types of users [1], and Chen, Xu, et al. [3] leverage user tastes from textual fashion reviews to highlight different image sections of the fashion item being recommended. Consequently, utilizing visual content as a means to explain recommendations can greatly enhance user understanding and satisfaction [11].

Within the idea of visual explanations, our particular approach of interest is the use of *user-generated images* to provide the explanations, avoiding a need for auxiliary information (e.g. text) to distil user tastes or a manual selection of creation of the images, thus yielding more organic explanations and improving the self-sustainability and scalability of the explainable methodology.

Leveraging user-created images is a promising but particularly challenging task: in the case of textual contents, a textual explanation may be associated with multiple users or items (e.g. the phrase “great visual effects” in movie reviews), which can help in tackling data sparsity [13]. User-created visual explanations (e.g. an image taken in a restaurant), however, are unique to each user and item, making it difficult for a model to distil user tastes. This challenge has been tackled by both ELVis [6] and MF-ELVis [15], which model and solve the explanation problem as a Learning to Rank (LTR) authorship task, predicting the best explanations of a (*user*, *item*) recommendation as a ranking of the images of the item most likely to have been authored by the user.

While explainability is crucial, it should not come at the expense of sustainability and model compactness. AI and Deep Learning models are known to consume significant computational resources, resulting in substantial carbon emissions and large model sizes; these environmental concerns highlight the need to strike a balance between model efficiency and explainability [20] [4]. Although ELVis is able to provide a high degree of explainability to an RS by leveraging user-created images, it achieves this by means of a Deep Learning-oriented architecture with a cost comparable to the Recommender System itself; MF-ELVis accomplishes a notable reduction in training carbon emissions and training time through a simpler latent Matrix Factorization architecture, but increases the model size four-fold in order to maintain competitiveness with ELVis [15].

In this work we introduce BRIE (Bayesian Ranking of Images for Explainability), a novel model designed to explain the outputs of Recommender Systems using existing images uploaded by the users themselves. BRIE addresses the aforementioned challenges not only surpassing the performances of the state-of-the-art models, ELVis and MF-ELVis, but also achieving higher efficiency and drastically improving model compactness. By adopting a training goal closer to the Learning to Rank authorship prediction task, namely the Bayesian Pairwise Ranking, BRIE learns to explain recommendations while minimizing carbon emissions, training time, and model size, showcasing that explainability can be achieved without sacrificing sustainability or compactness.

The primary contributions of this research are threefold:

- Firstly, we introduce, design and implement BRIE, a novel model that leverages existing user-uploaded images to provide visually interpretable explanations for Recommender System outputs. By incorporating the most adequate user content created by users themselves, BRIE seeks to optimize user understanding, trust, and engagement.
- Secondly, BRIE outperforms state-of-the-art models of the task, like ELVis and MF-ELVis, by adopting a training goal closer to the Learning to Rank task. This allows BRIE to achieve higher performance in six real-world datasets for image-driven explanation of recommendations.
- Lastly, BRIE addresses the inherent issue of sustainability in Explainable AI by minimizing carbon emissions, training time and particularly model size, ensuring that explainability can be achieved without sacrificing the efficiency of the explained model.

The structure of the paper is organized as follows. In Section 2, we introduce the visual explanations ranking task, discuss existing models (ELVis and MF-ELVis), and explore the choice of learning goals in explanation ranking tasks. Section 3 presents BRIE, our proposed algorithm that utilizes Bayesian Pairwise Ranking Paradigm for the task. Section 4 describes the experimental setup, including real-world datasets, performance and efficiency evaluation metrics, and implementation details. In Section 5, we present and discuss the performance of BRIE compared to state-of-the-art approaches and baselines. Finally, Section 6 summarizes the contributions and implications of BRIE in terms of explainability, efficiency, and sustainability.

2 BACKGROUND

2.1 Problem Formulation

In this subsection, we provide a formalization of the problem at hand: predicting the most suitable visual contents (photographs or images) to explain item recommendations to users made by any Recommender System or preceding information filtering algorithm. Let \mathcal{U} denote the set of users, \mathcal{I} denote the set of items, and \mathcal{P} denote the set of photographs of the items uploaded by users.

Our objective is then to predict the most suitable photographs that effectively are able to explain the recommendation of an item to a user. Our available information to do so (the “historical interactions” between \mathcal{U} , \mathcal{I} and \mathcal{P}) forms a set of *triads* as $\mathcal{D} = \{(u, i, p)\}$, where each triad represents a user $u \in \mathcal{U}$ interacting with an item $i \in \mathcal{I}$ by uploading the photograph $p \in \mathcal{P}$; it is then reasonable to state that p includes features of i that are relevant to the user u , and therefore would be a good explanation of the item i to user u .

The utilization of user-uploaded photographs as explanations for items introduces certain considerations that need to be addressed. Specifically, in most data contexts, each photograph is deemed a plausible explanation solely for the item it represents or is associated with, such as photographs depicting a hotel room or images found in product reviews. It is also important to note that \mathcal{D} contains only one triad for each photo $p \in \mathcal{P}$, even if a photo can be a relevant explanation for multiple users.

Therefore, leveraging user-generated item images as visual explanations poses two main challenges: 1) extracting meaningful latent information from photographs, given their limited association with multiple users and items, and 2) addressing data sparsity in real-world datasets where the available set of photographs \mathcal{P} may be insufficient compared to the set of users \mathcal{U} .

However, it is important to note that any photograph $p \notin \mathcal{P}_i$, i.e., any photograph that does not correspond to item i , can be readily disregarded as a plausible explanation for any recommendation of item i to a particular user. This simplifies the formulation of the task by narrowing the focus to only the photographs associated with the specific item under consideration.

Consequently, we can focus solely on the interaction matrix between users and photographs, denoted as $\mathbf{R} \in \mathbb{R}^{|\mathcal{U}| \times |\mathcal{P}|}$, where $|\mathcal{U}|$ and $|\mathcal{P}|$ denote the cardinalities of the user and photograph sets, respectively. Each element r_{up} of \mathbf{R} represents the relevance or preference score that user u assigns to photograph p . Our goal is to determine the optimal ranking function $f : \mathcal{U} \times \mathcal{I} \times \mathcal{P}_i \rightarrow \mathbb{R}$, which can assign a score to each photograph $p \in \mathcal{P}_i$ for a given user-item pair (u, i) . This ranking function reflects the probability that user u would have “authored” photograph p if they had interacted with item i . Thus, the higher the score assigned by f , the more suitable the photograph is as an explanation for the recommendation.

In particular, in order to identify the top explanation, we can find the photograph p^* that maximizes the ranking function f for a given user-item pair (u, i) :

$$p^* = \arg \max_{p \in \mathcal{P}_i} f(u, i, p)$$

In other words, p^* represents the photograph with the highest score according to f , indicating the most probable explanation for the recommendation of item i to user u .

As an explainability task, this problem assumes that the item i being recommended is already given in a previous step by a Recommender System or any other information filtering system that matches users with items, and therefore focuses on finding ranking function f that is best able to provide adequate explanations of any given user-item pair (u, i) .

2.2 ELVis and MF-ELVis

ELVis and MF-ELVis are the current state-of-the-art models for visual explainability through user-created images in Recommender Systems. In this subsection, we describe the functioning of these models and provide insights into their design choices. Fig. 1 depicts in detail the network topologies of both models.

2.2.1 ELVis. Díez et al. [6] propose in ELVis to capture the underlying patterns and preferences in the interactions between users and photographs by representing the interaction matrix \mathbf{R} as two latent matrices: the matrix of latent user preferences \mathbf{U} and the matrix of latent photograph features \mathbf{V}' .

ELVis generates a latent user vector $\mathbf{U}_u \in \mathbb{R}^d$ based on the user’s id, and obtains a latent photograph vector $\mathbf{V}'_p \in \mathbb{R}^d$ by projecting the ResNet-V2 [21] embedding $\mathbf{V}_p \in \mathbb{R}^{1536}$ of the original photograph into the latent feature subspace. The authors then propose to concatenate both vectors as \mathbf{x}_{up} . This concatenated vector is then passed through a multi-layer perceptron (MLP) g , which applies a series of non-linear transformations to the concatenated vector, such that

$$\hat{\mathbf{R}}_{up} = \sigma(g([\mathbf{U}_u; \mathbf{V}'_p])) \quad (1)$$

where σ is the sigmoid activation function (see Fig. 1), and the output $\hat{\mathbf{R}}_{up} \in [0, 1]$ is the predicted preference score for the (user, photograph) pair, or in other words, the adequacy of photograph p as an explanation of its associated item for user u .

The rationale behind ELVis’s design is based on using a **learned similarity function**, following the popular Neural Collaborative Filtering architecture [10]. The principle is that MLPs are general function approximators, so they should be -in theory- equally or more expressive than a fixed similarity function, such as a cosine similarity or dot product. Thus, by incorporating a learnable similarity function through the MLP, ELVis aims to capture complex and nuanced preferences, seeking a high model performance and providing adequate explanations to the user.

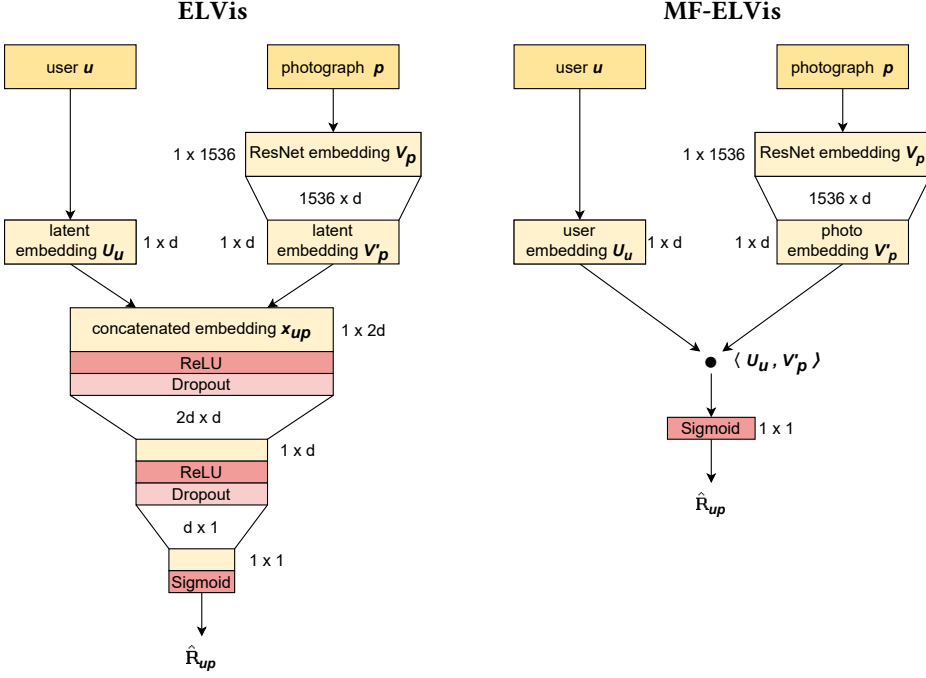


Fig. 1. Network topologies of ELVis and MF-ELVis. Both models take as inputs the identifiers of user u and the photograph p , and output the predicted preference \hat{R}_{up} of the user-photograph pair, i.e. how good is p as an explanation of a recommendation of its associated item for user u .

2.2.2 MF-ELVis. A later publication suggests MF-ELVis [15] to simplify the model architecture while maintaining performance. Similar to ELVis, MF-ELVis learns the latent user preference matrix U and item feature matrix V' . However, instead of an MLP, MF-ELVis uses a **fixed similarity function**, the inner product, to compute the similarity between the corresponding user vector U_u and photograph vector V'_p . For a given (user, photograph) pair, the preference score is calculated as

$$\hat{R}_{up} = \sigma \langle U_u, V'_p \rangle \quad (2)$$

The rationale for adopting the inner product in MF-ELVis is based on findings presented by Rendle et al. [17]. The study suggests that, in similarity-related tasks, the classic inner product can achieve performance comparable to an MLP while simplifying the model architecture. By leveraging the inner product operation, MF-ELVis significantly enhanced the time and carbon emissions required to train the model by accelerating the optimal convergence speed while maintaining a statistically competitive performance, albeit utilizing a much higher latent dimension d , thus increasing the overall model size.

2.3 How to learn explanation ranking tasks

One notable issue to address in the context of explanation ranking tasks is that the set of historical interactions, denoted as \mathcal{D} , contains only positive samples, which are triads representing good explanations of items to users, such that $R_{up} = 1$. However, in order to train a model that can learn the ranking function f , it is necessary to incorporate samples that represent suboptimal

explanations. The challenge then lies in determining an appropriate strategy for selecting negative samples.

Both ELVis and MF-ELVis address this issue by employing a random uniform negative sampling approach. Specifically, for each positive sample $(u, i, p) \in \mathcal{D}$, two random photos are assigned to user u and used during all the training as negative samples: a negative triad (u, i, p') (a photograph from the same restaurant as p originally uploaded by a different user u') and a negative triad (u, i', p') (a photograph originally uploaded by a different user u' in a restaurant other than i). This selection process is akin to the field of Positive-Unlabeled (PU) Learning, where the choice of random negative samples is a straightforward yet naive method [2]. While exploring more sophisticated negative sampling techniques is beyond the scope of this work, it is an important avenue for future research.

Another essential consideration in learning the ranking function is determining an appropriate loss function to minimize during training. ELVis and MF-ELVis adopt a binary classification formulation, utilizing binary cross-entropy (BCE) loss, which is commonly employed in classification tasks. The models are then evaluated using the original Learning to Rank “explanation rankings” framework. Although the choice of BCE loss can lead to reasonable results, it may not be the optimal approach for Learning to Rank tasks. One limitation is that BCE loss does not consider the relative ordering or the degree of difference between instances within the positive and negative classes, but ranking tasks require capturing the notion of preference and accurately modelling the relative ordering of samples. In other words, it is essential to distinguish between good explanations that are preferable to others, rather than simply classifying them as positive or negative.

Alternative methods have been developed specifically for optimizing models in Learning to Rank scenarios. One notable approach is Bayesian Pairwise Ranking (BPR), which provides an effective learning objective for pairwise ranking tasks [16]. BPR considers the relative preference between positive and negative samples and aims to maximize the probability of correctly ranking positive samples higher than negative ones, such as ranking good photographic explanations higher than worse ones.

3 PROPOSED ALGORITHM

In this section, we present BRIE (Bayesian Ranking of Images for Explainability), a novel model designed to address the limitations of ELVis and MF-ELVis in the context of the explanation of user-item pairs through user-created photographs. BRIE builds upon the strengths of MF-ELVis and incorporates additional improvements to enhance its performance and compactness.

3.1 Rationale for building BRIE

Acknowledging the limitations of ELVis and MF-ELVis we introduced in Section 2.3, BRIE seeks to optimize the learning goal specifically for explanation ranking tasks rather than using pure binary classification as a surrogate task. This approach should allow BRIE to better capture nuanced preferences of users.

Another key objective of BRIE is to enhance generalization by preventing the overfitting observed in MF-ELVis, as it can hinder the model’s ability to capture the underlying interactions between users and photographs accurately.

3.2 BRIE

BRIE’s topology closely resembles that of MF-ELVis, incorporating the improvements mentioned in the previous section. Let $\mathbf{U} \in \mathbb{R}^{|\mathcal{U}| \times d}$ represent the matrix of latent user embeddings, and $\mathbf{V}' \in \mathbb{R}^{|\mathcal{P}| \times d}$ represent the matrix of latent photograph embeddings. The latent user embedding \mathbf{U}_u

is extracted from the id of user u , and the latent photograph embedding \mathbf{V}'_p is obtained by projecting the ResNetv2 embedding of photograph p , as in ELVis and MF-ELVis.

To aid regularization and knowledge generalization, BRIE applies dropout to \mathbf{U}_u and \mathbf{V}'_p , resulting in modified embeddings denoted as $\widetilde{\mathbf{U}}_u$ and $\widetilde{\mathbf{V}}'_p$, respectively. The modified embeddings are then used to compute the dot product between $\widetilde{\mathbf{U}}_u$ and $\widetilde{\mathbf{V}}'_p$ as follows:

$$\hat{\mathbf{R}}_{up} = \langle \widetilde{\mathbf{U}}_u, \widetilde{\mathbf{V}}'_p \rangle \quad (3)$$

where again the output $\hat{\mathbf{R}}_{up} \in (-\infty, \infty)$ is the predicted preference score for the (user, photograph) pair. Note that, as we will not use a binary classification goal to learn the ranking task, we do not need to apply a sigmoid activation to map $\hat{\mathbf{R}}_{up}$ into the $[0, 1]$ range. Figure 2 can be referred to for an illustration of BRIE’s topology and data flow.

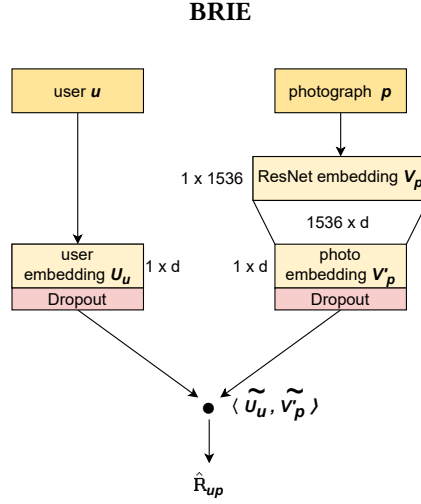


Fig. 2. Network topology of BRIE, which takes as inputs the identifiers of user u and the photograph p , and outputs the predicted preference $\hat{\mathbf{R}}_{up}$ of the user-photograph pair, i.e. how good is p as an explanation of a recommendation of its associated item for user u .

3.3 Explanation Ranking with BPR

BRIE utilizes the Bayesian Pairwise Ranking (BPR) algorithm for learning the ranking function f . BPR is tailored to optimize model weights by maximizing the probability of correctly ranking positive instances higher than negative instances. During training, at the start of each epoch, BRIE constructs an “extended” training set $\mathcal{D}^+ = (u, i, p, p_n)$ by uniformly sampling, for each $(u, i, p) \in \mathcal{D}$, a photograph p_n that is not part of $\mathcal{P}_u \subset \mathcal{P}$, i.e. a photograph from a purely random item and not taken by user u ; this is simpler than the selection method described in 2.3, but allows for much faster regeneration of negative samples between epochs.

If we formulate the BPR loss function over the entire extended dataset \mathcal{D}^+ , then it can be defined as:

$$\mathcal{L}_{\text{BPR}} = - \sum_{(u, i, p, p_n) \in \mathcal{D}^+} \log \left(\sigma(\hat{\mathbf{R}}_{up} - \hat{\mathbf{R}}_{up_n}) \right) \quad (4)$$

where σ represents the sigmoid function.

By minimizing the BPR loss function \mathcal{L}_{BPR} , BRIE learns an effective ranking function that captures the preferences of users in explanation ranking tasks, maximizing the ranking probability of positive instances over negative instances.

4 EXPERIMENTAL SETUP

4.1 Datasets

The datasets used in our experiments are derived from the original publication of ELVis by Diez et al. [6], comprising photographs uploaded by users in the context of restaurant reviews on TripAdvisor, a popular hospitality establishment reviewing website. We utilize public, real-world datasets from six different cities: Gijón, Barcelona, Madrid, New York, Paris, and London, in increasing the number of total photographs in the dataset, providing diverse contexts for evaluation both from a socio-cultural and a data perspective.

Each sample in the raw dataset consists of a triplet $(u, i, p) \in \mathcal{D}$, where u represents the user ID, i represents the restaurant ID, and p represents the photograph ID. The public datasets include the original train/validation/test partitions provided by the authors, ensuring replicability and comparability across different models.

For each test case, we have a photograph (p) that belongs to the user (u), which we refer to as the positive sample. The remaining photographs $p' \in (\mathcal{P}_i \setminus \mathcal{P}_u)$ of the same restaurant, contributed by different users, serve as negative samples. The goal of the model is to rank the positive sample (the user’s own photograph) as high as possible among the negative samples, indicating its relevance as an explanation. It is important to note that the positive samples in the test set correspond to users already present in the training set, ensuring a fair evaluation of the model’s ability to generalize to unseen user-photograph combinations.

To provide a comprehensive overview of the datasets’ characteristics, Table 1 summarizes key statistics, including the number of users, photographs, restaurants, and the overall sparsity of the datasets. We refer readers to the original ELVis publication [6] for more detailed information on the dataset extraction, characteristics, and partitioning.

Table 1. Basic statistics of each dataset.

City	Users	Restaurants	Photographs	Photos/User
Gijón	5,139	598	18,679	3.64
Barcelona	33,537	5,881	150,416	4.49
Madrid	43,628	6,810	203,905	4.67
New York	61,019	7,588	231,141	3.79
Paris	61,391	11,982	251,636	4.10
London	134,816	13,888	479,798	3.56

4.2 Compared Models

We compare BRIE against several baseline models from the State of the Art to evaluate its performance and effectiveness in explanation ranking tasks:

- **RND (Random):** Assigns a random preference $\hat{\mathbf{R}}_{u,p}$ to each (user, photograph) pair.
- **CNT (Centroid):** Estimates the preference of a (user, photograph) pair as the negative distance between the photograph ResNetv2 embedding \mathbf{V}_p and the centroid of the ResNetv2

embeddings of the photographs belonging to user u . Mathematically, the estimated preference can be represented as $\hat{\mathbf{R}}_{up} = -|\mathbf{V}_p - \frac{1}{\bar{\mathcal{P}}_u} \sum_{p' \in \mathcal{P}_u} \mathbf{V}_{p'}|$.

- **ELVis** [6]: Predicts the preference of a (user, photograph) pair applying a multi-layer perceptron g to the concatenation of the user's latent embedding \mathbf{U}_u and the photograph's latent embedding \mathbf{V}'_p as input. The estimated preference can be represented as $\hat{\mathbf{R}}_{up} = \sigma(g([\mathbf{U}_u; \mathbf{V}'_p])$.
- **MF-ELVis** [15]: MF-ELVis predicts the preference of a (user, photograph) pair using a dot product between the user's latent embedding \mathbf{U}_u and the photograph's latent embedding \mathbf{V}'_p . The estimated preference can be represented as $\hat{\mathbf{R}}_{up} = \sigma\langle \mathbf{U}_u, \mathbf{V}'_p \rangle$.

4.3 Evaluation Metrics

We evaluated the performance of the models using popular ranking metrics to assess their effectiveness in explanation ranking tasks, and compared their efficiency and compactness.

4.3.1 Performance Evaluation Metrics. Let \mathcal{T} be the set of test cases constructed as described in Section 4.1, where the predictions for each test case form a ranking $f(u, i)$ that orders the best photographs from restaurant i to explain a recommendation of the restaurant to user u . The performance evaluation metrics used in this work are as follows:

- **Mean Recall at k (MRecall@ k):**

$$\text{MRecall@}k = \frac{1}{|\mathcal{T}|} \sum_{f(u,i) \in \mathcal{T}} \text{TP}_{f(u,i)}(k) \quad (5)$$

where $\text{TP}_{f(u,i)}(k)$ is the number of true positive explanations at rank k for the ranking $f(u, i)$.

- **Mean Normalized Discounted Cumulative Gain at k (MNDCG@ k):**

$$\text{MNDCG@}k = \frac{1}{|\mathcal{T}|} \sum_{f(u,i) \in \mathcal{T}} \frac{\text{DCG}_{f(u,i)}(k)}{\text{IDCG}_{f(u,i)}(k)} \quad (6)$$

where $\text{DCG}_{f(u,i)}(k)$ is the discounted cumulative gain at rank k for the ranking $f(u, i)$, and $\text{IDCG}_{f(u,i)}(k)$ is the ideal discounted cumulative gain at rank k for the ranking $f(u, i)$.

- **Mean Area Under the ROC Curve (MAUC):**

$$\text{MAUC} = \frac{1}{|\mathcal{T}|} \sum_{f(u,i) \in \mathcal{T}} \text{AUC}_{f(u,i)} \quad (7)$$

where $\text{AUC}_{f(u,i)}$ is the area under the ROC curve for the ranking $f(u, i)$.

- **Median Percentile (MedPerc):**

$$\text{MedPerc} = \text{median} \left(\left\{ \frac{R_{f(u,i)}}{N_{f(u,i)}} \times 100 \mid f(u, i) \in \mathcal{T} \right\} \right) \quad (8)$$

where $R_{f(u,i)}$ is the position of the real positive sample (user's real photograph) in the ranking $f(u, i)$, and $N_{f(u,i)}$ is the total number of predictions for the ranking $f(u, i)$; therefore, the lower the percentile, the better the performance of the model.

These performance evaluation metrics provide a comprehensive assessment of the models' effectiveness in explanation ranking tasks. MRecall@ k and MNDCG@ k are computed with $k = 10$ for test cases where there are 10 or more photos to rank, and where the associated user has at least 10 photos in the training set, in order to ensure that we have sufficient per-user data to measure the performance of the models effectively. On the other hand, MAUC considers all test cases and users;

since AUC provides a comprehensive evaluation of the model’s ability to distinguish between good and bad explanations across various scenarios, by considering all test cases we capture the overall discriminative power of the models.

4.3.2 Efficiency and Compactness Metrics. In addition to the performance evaluation metrics, we also consider the following efficiency and compactness metrics:

- **Evolution of Test MAUC with Training Time and Carbon Emissions:** This analysis measures the time and carbon emissions required to train each model while tracking the MAUC during all the process, helping understand the trade-off between training resources and model effectiveness.
- **Inference Time and Energy Cost:** This metric estimates the time and carbon emissions required to utilize the model in a practical use case, simulating a final production environment. To do this, we track the aforementioned criteria as we obtain the models’ predictions for all the test cases in the test set of each dataset.
- **Impact of Number of Parameters in Test MAUC:** This comparison examines how the number of latent factors d affects the performance of the models.

All time and carbon emissions of the models are measured using the popular Codecarbon [19] package.

4.4 Implementation Details

4.4.1 Framework and Machine Configuration. To ensure reproducibility and provide a fair evaluation of all proposed models, we implemented a Python framework¹ using PyTorch-Lightning², a popular deep learning library that provides a high-level interface for training models with efficient use of computing resources.

All experiments, including model training and evaluation, were conducted on a dedicated machine with the following specifications:

- Processor: Intel Core i7-10700
- GPU: NVIDIA RTX 2060 Super
- RAM: 16GB
- Operating System: Windows 10

The machine was solely dedicated to training the models, ensuring optimal utilization of resources. Due to memory constraints produced by the large model sizes of ELVis and MF-ELVis, we employed different multiprocessing configurations during the training process for different datasets. Specifically, the models for Gijón, Barcelona, and Madrid were trained using 4 multiprocessing workers, while the models for New York and Paris utilized 2 workers. Models for London were trained without multiprocessing.

¹<https://github.com/Kominaru/BRIE>

²<https://www.pytorchlightning.ai/>

4.4.2 Model Hyperparameters. For ELVis³ and MF-ELVis⁴, the hyperparameters used were originally selected by the authors through a **grid search** in the validation sets of each dataset, identifying a specific configuration **per dataset**.

For BRIE, we performed **one random search** in the validation set of Barcelona, training 25 models inside the following hyperparameter space: latent factors (d) ranging from 4 to 1024, learning rate (lr) ranging from 10^{-3} to 10^{-5} , and dropout ranging from 0 to 0.8. A fixed batch size of 2^{14} was used, and an early stopping policy was implemented with a patience $p=5$, a delta $\delta=10^{-3}$, and a maximum of 100 epochs while tracking validation MAUC during training, as suggested by the BPR publication [16]. The Adam optimizer [12] was employed, and all model parameters were initialized using a Xavier distribution [8].

After a hyperparameter search on Barcelona’s validation set, we trained on all datasets with the selected configuration, without early stopping. We chose hyperparameters ($d=64$, $lr=10^{-3}$, dropout=0.75, 15 epochs) optimizing efficiency and compactness while consistently outperforming the State of the Art, prioritizing sustainability over marginal performance gains.

5 RESULTS AND DISCUSSION

In this section, we compare BRIE with state-of-the-art and baseline methods using the experimental setup described in Section 4. We evaluate the models’ performance using standard metrics, assess their efficiency and sustainability in terms of time and energy consumption during training and inference, and investigate the impact of the number of latent factors on model performance.

5.1 Performance comparison

Table 2 presents the performance of all models on the six datasets using three evaluation metrics (MRecall@10, MNDCG@10, MAUC). BRIE consistently outperforms other models in all metrics and datasets, indicating its superior ability to provide explanations with user-created images. On average, BRIE achieves a relative improvement of approximately 7.5% over the second-best method in terms of MAUC, the most comprehensive metric. This suggests that BRIE’s utilization of Bayesian Pairwise Ranking as a learning goal effectively captures nuanced preferences and interactions between users and photographs, and is as such a learning goal better suited for explanation ranking tasks than surrogate classification goals.

Table 2. Performance summary of all models across the six selected datasets. For each city and metric, the best model is boldfaced, and the second best model is underlined.

	Gijón			Barcelona			Madrid		
	MRecall@10	MNDCG@10	MAUC	MRecall@10	MNDCG@10	MAUC	MRecall@10	MNDCG@10	MAUC
RND	0.373	0.185	0.487	0.409	0.186	0.502	0.374	0.171	0.499
CNT	0.464	0.218	0.546	0.443	0.219	0.554	0.420	0.203	0.557
ELVis	0.521	0.262	<u>0.596</u>	<u>0.597</u>	<u>0.327</u>	<u>0.631</u>	<u>0.572</u>	<u>0.314</u>	<u>0.638</u>
MF-ELVis	0.538	0.285	0.592	0.557	0.293	0.596	0.528	0.279	0.601
BRIE	0.607	0.333	0.643	0.630	0.368	0.663	0.612	0.348	0.673

	Newyork			Paris			London		
	MRecall@10	MNDCG@10	MAUC	MRecall@10	MNDCG@10	MAUC	MRecall@10	MNDCG@10	MAUC
RND	0.374	0.168	0.502	0.459	0.209	0.502	0.342	0.155	0.500
CNT	0.431	0.217	0.563	0.499	0.245	0.557	0.400	0.200	0.562
ELVis	0.553	<u>0.304</u>	<u>0.637</u>	<u>0.643</u>	<u>0.352</u>	<u>0.630</u>	0.530	<u>0.293</u>	<u>0.629</u>
MF-ELVis	0.516	0.276	0.602	0.606	0.323	0.596	<u>0.531</u>	0.267	0.597
BRIE	0.598	0.341	0.677	0.669	0.391	0.666	0.563	0.318	0.665

³<https://github.com/pablo-pnunez/ELVis>

⁴<https://github.com/Kominaru/tfg-komi>

While ELVis aims to achieve high performance by leveraging the expressiveness of the MLP architecture, it falls short in comparison to BRIE. In contrast, MF-ELVis simplifies the model by using the inner product as a fixed similarity function between user and photograph vectors; while this approach accelerates training and reduces carbon emissions, it compromises the model’s expressiveness compared to ELVis and increases overfitting. As a result, MF-ELVis lags behind ELVis in performance and both methods fall behind BRIE, as they use binary classification as a surrogate learning goal, which is suboptimal for modelling the explanation ranking task.

The median percentile analysis, as shown in Figure 3, provides insights into the models’ performance with varying user information availability. Generally, higher activity thresholds (i.e. more available information about each user) lead to improved performance for all models (except Random and CNT). While it is challenging to compare BRIE and ELVis in scenarios with abundant user information, BRIE consistently outperforms all models when user information is scarce. This suggests BRIE’s strength in providing explanations with limited user data, making it a robust choice for diverse scenarios.

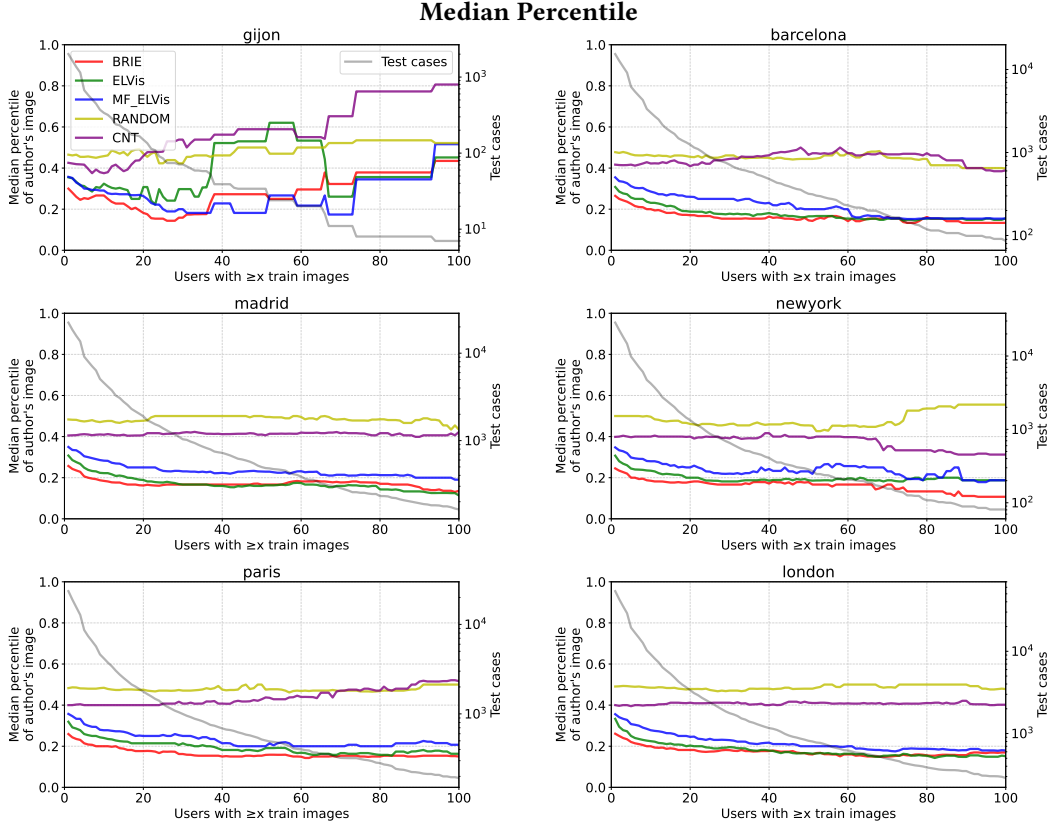


Fig. 3. Effect of the amount of information per user on the median percentile of all models. Each subfigure displays the median percentile as a function of the minimum activity threshold, i.e. the minimum required number of photographs by the user present in the training set. The x-axis represents this minimum activity threshold, while the y-axis displays the median percentile. The count of available test cases for each minimum activity threshold is also provided as an aid in assessing the statistical significance of the results. Note that a lower percentile of the user’s image implies a better performance of the model.

In summary, BRIE consistently outperforms ELVis, MF-ELVis, and the random and CNT baseline in all analyzed metrics and datasets. The model’s ability to capture nuanced preferences and interactions, coupled with its efficient and well-suited learning goal, contributes to its superior performance. The median percentile evaluation further confirms the robustness of BRIE’s performance across different scenarios of user information availability.

5.2 Efficiency and sustainability comparison

In this subsection we compare the efficiency and sustainability of the BRIE, ELVis, and MF-ELVis by comparing the evolution of AUC versus training time and CO₂ emissions for all models and datasets, as well as inference times and CO₂ emissions. Both training and inference are performed using GPU acceleration, and the final models used for reporting the results in Table 2 are considered.

Figure 4 compares AUC evolution versus training time and CO₂ emissions for the different models. At the end of the training process, BRIE emits approximately 75% less CO₂ than ELVis and 50% less than MF-ELVis, the current most sustainable model. Moreover, BRIE requires around three times less training time than ELVis in all cities, tying MF-ELVis as the model with the fastest training. The figure also reveals an interesting insight: BRIE consistently outperforms ELVis and MF-ELVis no matter the training time and emitted CO₂, i.e. for any given training time or CO₂ emissions goal, BRIE can achieve higher performance compared to the other models. Alternatively, if a specific performance goal is set, BRIE can attain it faster and with lower CO₂ emissions.

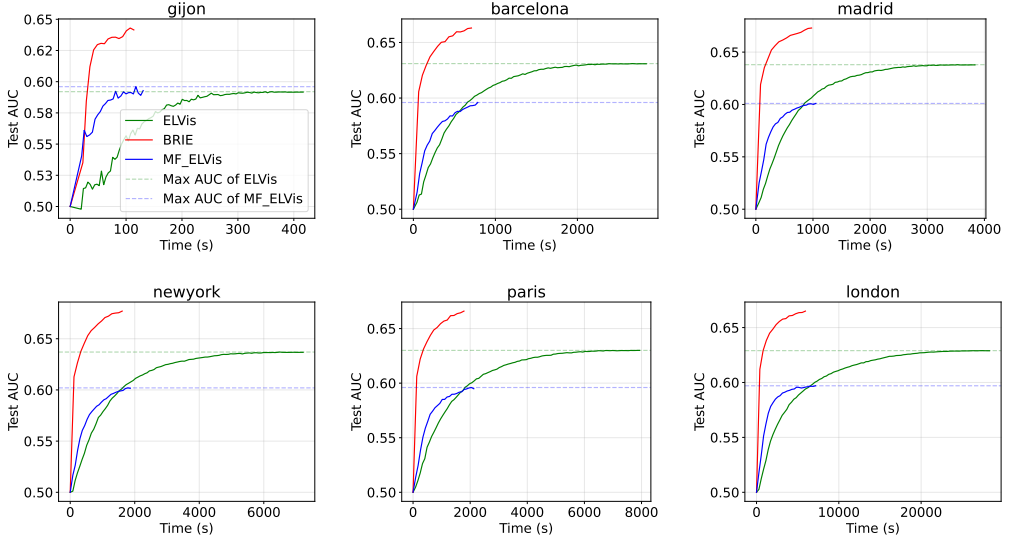
With respect to inference, Figure 5 shows BRIE and MF-ELVis present no significant variation and are consistently around two times faster than ELVis. Furthermore, BRIE emits 50% less CO₂ during inference compared to both MF-ELVis and ELVis.

Overall, these findings can be attributed to several factors. Firstly, BRIE’s adoption of the Bayesian Pairwise Ranking (BPR) learning goal enables it to achieve higher performance early in the training process. Secondly, the complexity and resource requirements of the use of an MLP as a learned similarity function in ELVis incur penalties in terms of training and inference CO₂ emissions and time compared to BRIE’s fixed similarity function based on dot product.

Moreover, the high embedding dimension (number of factors d) employed in MF-ELVis ($d = 1024$) and ELVis ($d = 256$) leads to a substantial penalty in terms of emissions. Notably, although BRIE requires two different images p and p_n in each training sample instead of only p , the training times and emissions for BRIE are comparable to MF-ELVis’s, and the inference emissions of MF-ELVis are in some cases higher than those of ELVis. It is also worth noting that the use of CUDA in this experiment mitigates larger penalties associated with the high embedding dimensions of ELVis and MF-ELVis, as these would be highly inefficient to handle using CPU only, in contrast with the smaller embeddings managed by BRIE.

To summarize, BRIE not only achieves higher performances but also provides higher sustainability than existing state-of-the-art models, establishing a lead early in the training process and a high inference efficiency. The penalties associated with ELVis’s MLP-based similarity function and MF-ELVis’s high embedding dimension highlight the importance of not neglecting efficiency and sustainability; by considering these factors, we can develop environmentally friendly and resource-efficient models for generating personalized explanations in recommendation systems.

Training Time vs. Test AUC



CO₂ Emissions vs. Test AUC

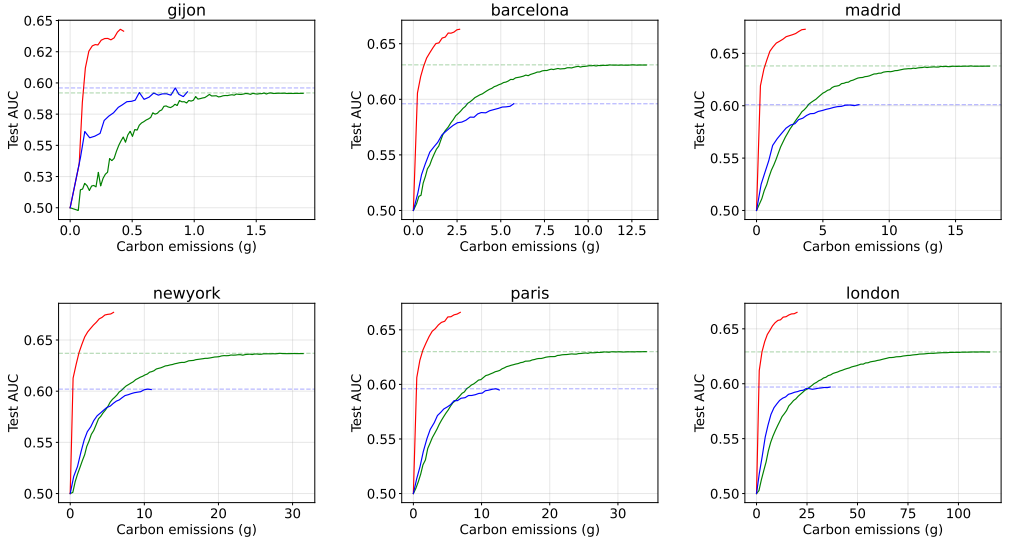


Fig. 4. Comparison of Time vs. AUC and Carbon Emissions vs. AUC during training for the trainable models (ELViS, MF-ELViS, and BRIE) across different cities. Each subfigure in the top section of the figure displays the time vs. AUC figures, showing how the AUC performance evolves over time for each model. Each subfigure in the bottom section shows the carbon emissions vs. AUC figures, illustrating the relationship between carbon emissions and AUC performance during training.

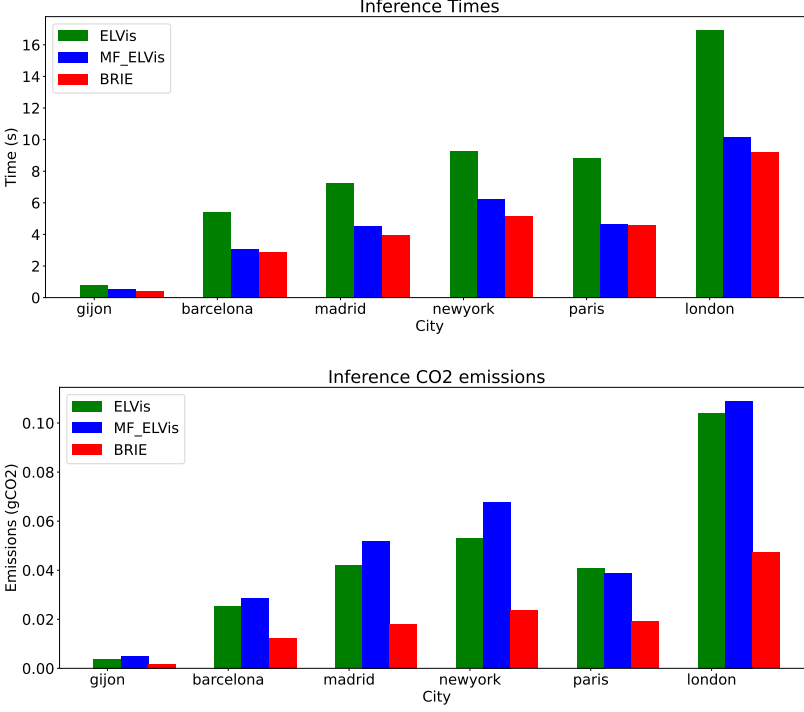


Fig. 5. Comparison of inference times (top) and inference emissions (bottom) for different models across the six datasets. The results represent the average inference costs of predicting the test set in each dataset, averaged over 50 runs. GPU acceleration using CUDA was employed for both training and inference.

5.3 Compactness comparison

In this section, we examine how the size of the models, particularly the choice of the number of latent factors (d), the main contributor to model size, influences their performance. Figure 6 presents the results of the compactness comparison, with each subfigure representing a specific city. Test AUC values for all three models (ELVis, MF-ELVis, BRIE) and varying numbers of latent factors d (4 to 1024, in powers of 2) are plotted.

The figure reveals several notable observations across all datasets:

- The performance of MF-ELVis and BRIE remains relatively consistent even with a small number of latent factors.
- ELVis experiences a sharp decline in performance as the number of learnt latent factors decreases. In fact, when d is as small as 4, ELVis performs poorly, almost on par with random predictions.
- BRIE consistently outperforms MF-ELVis regardless of the number of latent factors used, and achieves generally better results than ELVis even with a low d . In some cases, BRIE with $d = 4$ can even outperform ELVis with $d = 1024$.

The results suggest that MF-ELVis and BRIE demonstrate a higher level of compactness compared to ELVis. The ability of MF-ELVis and BRIE to perform well with a smaller number of latent factors can probably be attributed to the choice of a fixed similarity function in order to compute the

Number of latent factors d vs. Test AUC

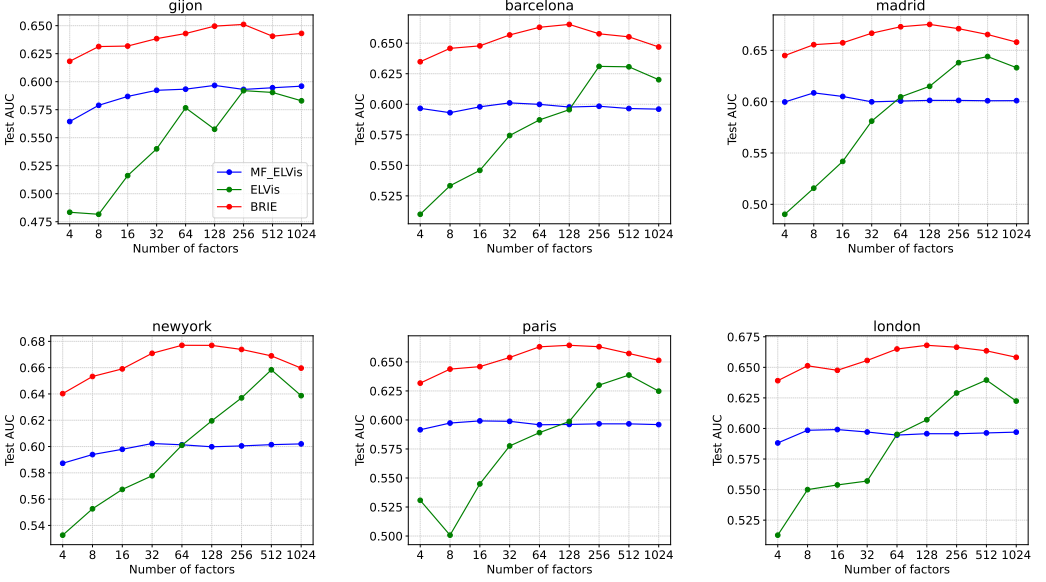


Fig. 6. Impact of the number of factors d (size of the latent embeddings of users and photographs) on the performance of the three trainable models (ELVis, MF-ELVis, BRIE), in terms of the Test MAUC, the most global metric. Each subfigure corresponds to a specific city: Gijón, Barcelona, Madrid, New York, Paris, and London. The x-axis represents the number of factors, ranging from 4 to 1024, while the y-axis shows the Test MAUC value.

suitability of the photograph as an explanation for the user. In contrast, ELVis, which relies on a learned MLP as the similarity function, appears to be more sensitive to the reduction in the number of latent factors, leading to a significant performance drop, likely due to the degradation of information through the series of dropout, activation and dense layers that form the MLP.

These findings demonstrate the robustness of MF-ELVis and BRIE across varying numbers of latent factors. These models exhibit consistent performance even with a smaller d , while ELVis experiences a substantial degradation in performance as d decreases. Therefore, the compact nature of BRIE makes it an attractive option for applications where model size and computational efficiency are of paramount importance.

6 CONCLUSIONS

In this work, we have explored the generation of personalized explanations in recommendation systems, specifically focusing on explaining recommendations using user-created photographs. Our approach, BRIE, has shown promising results in addressing the limitations of existing models: by leveraging the Bayesian Pairwise Ranking (BPR) as a more adequate learning goal, BRIE achieves superior performance even early in training, and demonstrates remarkable efficiency, emitting significantly fewer carbon emissions during training and inference compared to other state-of-the-art models. Moreover, BRIE maintains its effectiveness even with reduced computational resources and a drastic decrease in the total model size. Our findings highlight the need for improved models that excel in terms of performance without sacrificing efficiency and sustainability; BRIE represents a clear step forward in this direction.

Moving forward, there are important avenues for future work. Firstly, we can explore methods for improved negative sample selection during training to enhance the model’s ability to discriminate between positive and negative instances; selecting only “reliable negatives” for training has the potential to lead to improved performance and more reliable explanations. Secondly, addressing the “cold start” problem is crucial, enabling BRIE to provide personalized explanations to new users efficiently. Techniques such as transfer learning can be explored for this purpose, as currently the system needs to be partially re-trained to provide explanations to new users.

Lastly, ensuring the scalability of BRIE is important as recommendation systems deal with increasingly larger datasets and user bases, and the model sizes of BRIE and other models scale linearly with the number of unique users. Investigating methods to optimize the model’s scalability and resource utilization will enhance its practical applicability. By addressing these limitations and exploring new possibilities, we can enhance transparency and user trust, and ultimately provide more valuable explanations for recommendations in various domains.

ACKNOWLEDGMENTS

This research project has been supported by the National Plan for Scientific and Technical Research and Innovation of the Spanish Government (Grant PID2019-109238GB-C22), by the Spanish Ministry of Science and Innovation (Grant FPU21/05783), and by the Xunta de Galicia (Grant ED431C 2022/44) with the European Union ERDF funds. CITIC, as Research Center accredited by Galician University System, is funded by “Consellería de Cultura, Educación e Universidade from Xunta de Galicia”, supported in an 80% through ERDF Operational Programme Galicia 2014-2020, and the remaining 20% by “Secretaría Xeral de Universidades” (Grant ED431G 2019/01).

REFERENCES

- [1] Fernando Amat. 2023. Artwork Personalization at Netflix. <https://research.netflix.com/publication/Artwork%20Personalization%20at%20Netflix>
- [2] Jessa Bekker and Jesse Davis. 2020. Learning from positive and unlabeled data: A survey. *Machine Learning* 109 (2020), 719–760.
- [3] Xu Chen, Hanxiong Chen, Hongteng Xu, Yongfeng Zhang, Yixin Cao, Zheng Qin, and Hongyuan Zha. 2019. Personalized Fashion Recommendation with Visual Explanations Based on Multimodal Attention Network: Towards Visually Explainable Recommendation. In *Proceedings of the 42nd International ACM SIGIR Conference on Research and Development in Information Retrieval* (Paris, France) (SIGIR’19). Association for Computing Machinery, New York, NY, USA, 765–774. <https://doi.org/10.1145/3331184.3331254>
- [4] Yu Cheng, Duo Wang, Pan Zhou, and Tao Zhang. 2018. Model compression and acceleration for deep neural networks: The principles, progress, and challenges. *IEEE Signal Processing Magazine* 35, 1 (2018), 126–136.
- [5] Federal Trade Commission. 2018. Big Data: A Tool for Inclusion or Exclusion? Understanding the Issues. <https://www.ftc.gov/system/files/documents/reports/big-data-tool-inclusion-or-exclusion-understanding-issues/170106big-data-rpt.pdf>
- [6] Jorge Diez, Pablo Perez-Nunez, Oscar Luaces, Beatriz Remeseiro, and Antonio Bahamonde. 2020. Towards explainable personalized recommendations by learning from users’ photos. *Information Sciences* 520 (2020), 416–430.
- [7] Finale Doshi-Velez, Mason Kortz, Ryan Budish, Chris Bavitz, Sam Gershman, David O’Brien, Kate Scott, Stuart Schieber, James Waldo, David Weinberger, Adrian Weller, and Alexandra Wood. 2019. Accountability of AI Under the Law: The Role of Explanation. arXiv:1711.01134 [cs.AI]
- [8] Xavier Glorot and Yoshua Bengio. 2010. Understanding the difficulty of training deep feedforward neural networks. In *Proceedings of the thirteenth international conference on artificial intelligence and statistics*. JMLR Workshop and Conference Proceedings, 249–256.
- [9] Pascal Hamm, Michael Klesel, Patricia Coberger, and H Felix Wittmann. 2023. Explanation matters: An experimental study on explainable AI. *Electronic Markets* 33, 1 (2023), 1–21.
- [10] Xiangnan He, Lizi Liao, Hanwang Zhang, Liqiang Nie, Xia Hu, and Tat-Seng Chua. 2017. Neural Collaborative Filtering. In *Proceedings of the 26th International Conference on World Wide Web* (Perth, Australia) (WWW ’17). International World Wide Web Conferences Steering Committee, Republic and Canton of Geneva, CHE, 173–182. <https://doi.org/10.1145/3038912.3052569>

- [11] Lisa Anne Hendricks, Zeynep Akata, Marcus Rohrbach, Jeff Donahue, Bernt Schiele, and Trevor Darrell. 2016. Generating Visual Explanations. In *Computer Vision – ECCV 2016*, Bastian Leibe, Jiri Matas, Nicu Sebe, and Max Welling (Eds.). Springer International Publishing, Cham, 3–19.
- [12] Diederik P. Kingma and Jimmy Ba. 2017. Adam: A Method for Stochastic Optimization. arXiv:1412.6980 [cs.LG]
- [13] Lei Li, Yongfeng Zhang, and Li Chen. 2023. On the relationship between explanation and recommendation: Learning to rank explanations for improved performance. *ACM Transactions on Intelligent Systems and Technology* 14, 2 (2023), 1–24.
- [14] High-Level Expert Group on Artificial Intelligence. 2019. Ethics Guidelines for Trustworthy AI. <https://ec.europa.eu/digital-single-market/en/news/ethics-guidelines-trustworthy-ai>
- [15] Jorge Paz-Ruza, Carlos Eiras-Franco, Bertha Guijarro-Berdinas, and Amparo Alonso-Betanzos. 2022. Sustainable Personalisation and Explainability in Dyadic Data Systems. *Procedia Computer Science* 207 (2022), 1017–1026.
- [16] Steffen Rendle, Christoph Freudenthaler, Zeno Gantner, and Lars Schmidt-Thieme. 2009. BPR: Bayesian Personalized Ranking from Implicit Feedback. In *Proceedings of the Twenty-Fifth Conference on Uncertainty in Artificial Intelligence* (Montreal, Quebec, Canada) (UAI '09). AUAI Press, Arlington, Virginia, USA, 452–461.
- [17] Steffen Rendle, Walid Krichene, Li Zhang, and John Anderson. 2020. Neural Collaborative Filtering vs. Matrix Factorization Revisited. In *Proceedings of the 14th ACM Conference on Recommender Systems* (Virtual Event, Brazil) (RecSys '20). Association for Computing Machinery, New York, NY, USA, 240–248. <https://doi.org/10.1145/3383313.3412488>
- [18] Marco Tulio Ribeiro, Sameer Singh, and Carlos Guestrin. 2016. "Why Should I Trust You?": Explaining the Predictions of Any Classifier. In *Proceedings of the 22nd ACM SIGKDD International Conference on Knowledge Discovery and Data Mining* (San Francisco, California, USA) (KDD '16). Association for Computing Machinery, New York, NY, USA, 1135–1144. <https://doi.org/10.1145/2939672.2939778>
- [19] Victor Schmidt, Kamal Goyal, Aditya Joshi, Boris Feld, Liam Conell, Nikolas Laskaris, Doug Blank, Jonathan Wilson, Sorelle Friedler, and Sasha Luccioni. 2021. CodeCarbon: estimate and track carbon emissions from machine learning computing. , 20 pages.
- [20] Emma Strubell, Ananya Ganesh, and Andrew McCallum. 2020. Energy and Policy Considerations for Modern Deep Learning Research. *Proceedings of the AAAI Conference on Artificial Intelligence* 34, 09 (Apr. 2020), 13693–13696. <https://doi.org/10.1609/aaai.v34i09.7123>
- [21] Christian Szegedy, Sergey Ioffe, Vincent Vanhoucke, and Alexander A. Alemi. 2017. Inception-v4, Inception-ResNet and the Impact of Residual Connections on Learning. (2017), 4278–4284.
- [22] European Union. 2016. General Data Protection Regulation (GDPR). <https://gdpr-info.eu/>
- [23] Matthew D. Zeiler and Rob Fergus. 2014. Visualizing and Understanding Convolutional Networks. In *Computer Vision – ECCV 2014*, David Fleet, Tomas Pajdla, Bernt Schiele, and Tinne Tuytelaars (Eds.). Springer International Publishing, Cham, 818–833.
- [24] Yongfeng Zhang, Xu Chen, et al. 2020. Explainable recommendation: A survey and new perspectives. *Foundations and Trends® in Information Retrieval* 14, 1 (2020), 1–101.